ISSN 1674-1056
http://cpb.iphy.ac.cn
http://iopscience.iop.org/cpb
中国物理 B
Chinese Physics
中国物理
Chinese Physics B

Tunneling exits of H_2^+ in strong laser fields

Zhao-Han Zhang(张兆涵), Feng He(何峰)

Citation: Chin. Phys. B . 2018, 27(10): 104203. **doi:** 10.1088/1674-1056/27/10/104203

Journal homepage: http://cpb.iphy.ac.cn; http://iopscience.iop.org/cpb

What follows is a list of articles you may be interested in

Femtosecond laser user facility for application research on ultrafast science

Zhaohua Wang(王兆华), Shaobo Fang(方少波), Hao Teng(滕浩), Hainian Han(韩海年), Xinkui He(贺新奎), Zhiyi Wei(魏志义)

Chin. Phys. B . 2018, 27(7): 074204. **doi:** 10.1088/1674-1056/27/7/074204

Two-dimensional materials for ultrafast lasers

Fengqiu Wang(王枫秋)

Chin. Phys. B . 2017, 26(3): 034202. **doi:** 10.1088/1674-1056/26/3/034202

Characteristic of femtosecond laser-pulsed digital holography

Shi Bing-Chuan, Wang Xiao-Lei, Guo Wen-Gang, Song Li-Pei

Chin. Phys. B . 2015, 24(8): 084202. **doi:** 10.1088/1674-1056/24/8/084202

Radio-frequency compressed electron pulse-width characterization by cross-correlation between electron bunches and laser-induced plasma

Li Jing, Pei Min-Jie, Qi Da-Long, Qi Ying-Peng, Yang Yan, Sun Zhen-Rong

Chin. Phys. B . 2014, 23(12): 124209. **doi:** 10.1088/1674-1056/23/12/124209

Low temperature enhancement of alignment-induced spectral broadening of femtosecond laser pulses

Wang Fei, Jiang Hong-Bing, Gong Qi-Huang

Chin. Phys. B . 2014, 23(1): 014201. **doi:** 10.1088/1674-1056/23/1/014201

Tunneling exits of H_2^+ in strong laser fields*

Zhao-Han Zhang(张兆涵)[1] and Feng He(何峰)[1,2†]

[1] Key Laboratory for Laser Plasmas (Ministry of Education) and School of Physics and Astronomy, Shanghai Jiao Tong University, Shanghai 200240, China

[2] Collaborative Innovation Center of IFSA (CICIFSA), Shanghai Jiao Tong University, Shanghai 200240, China

(Received 11 April 2018; revised manuscript received 28 May 2018; published online 10 September 2018)

Different from atoms, the multicenter of the Coulombic potentials in molecules makes the tunneling ionization complex, and the electron tunnels out the laser-dressed Coulomb potential with a complex structure. We study tunneling exits of H_2^+ at large internuclear distance in strong laser fields by numerically simulating the time-dependent Schrödinger equation plus a classical backward propagation of the ionized wave packet. This study strengthens the understanding of molecular tunneling ionization in strong laser fields.

Keywords: ultrafast, tunneling, laser, hydrogen molecular ion

PACS: 42.50.Hz 42.65.Re 82.30.Lp **DOI:** 10.1088/1674-1056/27/10/104203

1. Introduction

Ionization of atoms and molecules in strong laser fields is overwhelmingly important.[1,2] Ionization carries the information of the target structures, which may be used to image atoms or molecules. The photoelectron probability and momentum spectrum allow us to understand the ultrafast dynamics during the ionization. Ionization also works as the first step for producing the unprecedented ultrashort photon sources.[3,4] Ionization can be understood with different pictures according to the Keldysh parameters $\gamma = \sqrt{I_p/2U_p}$,[5] where I_p is the ionization potential and U_p is the averaged quiver energy for an electron in a plane electromagnetic wave. When $\gamma \gg 1$, the electron absorbs multiple photons and escapes, carrying the energy $n\hbar\omega - I_p$. On the other hand, when $\gamma \ll 1$, the Coulomb potential is strongly suppressed, and the bound electron has enough time to tunnel through the laser-dressed Coulomb barrier with the final momentum equating to the opposite laser vector potential at the moment when the electron tunnels out if the Coulomb potential is neglected.

Because of the high nonlinearity, the tunneling process is very complex and has attracted a lot of attention over the past few decades. The theoretical description of tunneling is crucial for ultimately explaining the photoelectron momentum distribution. The static tunneling ionization of atoms can be satisfactorily predicted by the Ammosov–Delone–Keldysh (ADK) theory,[6,7] and the quasi-static tunneling ionization of atoms can be described by the PPT formula.[8] Tong *et al.* extended the atomic ADK theory to the molecular ADK theory, which can explain the suppression of the ionization of O_2 compared to the accompanied Xe atom.[9] More and more studies explored that the nonadiabatic effect is important during the tunneling ionization,[10,11] and thus the tunneling exit as well as the photoelectron momentum distribution at tunneling need to be revisited.

Among several methods, the backward propagation developed by Ni *et al.*[12] can describe the tunneling characters accurately, such as the tunneling time, the tunneling exit, and the photoelectron momentum distribution at tunneling. This method has been used to exclude the concept of the tunneling time,[13] to explain the different ionization probabilities of atoms carrying different angular momenta.[14] Compared to atoms, molecular tunneling processes are more complex due to multiple Coulomb centers. In this paper, we numerically simulate the time-dependent Schrödinger equation (TDSE) to obtain the ionized electron wave packet, which will be backward propagated in order to extract the tunneling characters in the tunneling ionization of H_2^+ in strong laser fields. Our simulation results give a clear picture of how the electron tunnels out the spatially complex Coulomb potential, and how the electron flies away from the two nuclei in strong laser fields.

2. Numerical models

2.1. TDSE simulation

As the simplest molecule in nature, H_2^+ works as a prototype to explore the molecular dynamics in strong laser fields. In our model, the internuclear distance is fixed during the ionization, which is proper since the nuclei move much slower than the electron. We confine the dynamics in the plane determined by the molecular axis and the laser polarization direction. The TDSE is (atomic units are used unless stated other-

*Project supported by National Natural Science Foundation of China (Grant Nos. 11574205, 11327902, and 11421064), the Innovation Program of Shanghai Municipal Education Commission (Grant No. 2017-01-07-00-02-E00034).

†Corresponding author. E-mail: fhe@sjtu.edu.cn

© 2018 Chinese Physical Society and IOP Publishing Ltd

wise)

$$\mathrm{i}\frac{\partial}{\partial t}\Psi(x,y,t)=\left(-\frac{1}{2}\nabla^2+V(x,y)+xE(t)\right)\Psi(x,y,t), \quad (1)$$

where the field-free potential of H_2^+ is

$$V(x,y) = -\frac{1}{\sqrt{(x+R/2)^2+y^2+s}} - \frac{1}{\sqrt{(x-R/2)^2+y^2+s}}. \quad (2)$$

In Eq. (2), the soft-core parameter $s=0.64$ is determined by matching the simulated ground state energy with the real one. This model has been used to observe the Coulomb action on the photoelectron angular distribution[15] and the photon momentum transfer to the electron longitudinal momentum.[16] We use an electric field that has a duration of only half a cycle to tunnel ionize the atom,

$$E=-E_0\sin^3(\omega t), \quad 0<t<\pi/\omega. \quad (3)$$

The amplitude E_0 is 0.025 a.u., (the unit a.u. is short for atomic unit), $\omega=0.0304$ a.u., and the corresponding Keldysh parameter is $\gamma\approx 1.2$. Such an electric field kills the rescattering process, and makes it easier to analyze the tunneling process. Since the ionization driven by the laser pulse whose polarization axis is perpendicular to the molecular axis presents more characters of atomic ionization, we only consider the case that the laser polarization axis is parallel to the molecular axis. Please note that the tunneling and multiphoton ionization is not necessary to be divided by $\gamma=1$, and some studies have confirmed that tunneling pictures still work for $\gamma=3$.[17] The field-dressed Coulomb potential at the peak of the electric field is shown in Fig. 1.

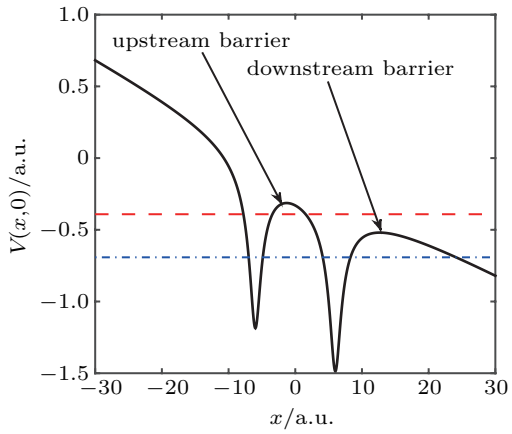


Fig. 1. (color online) The field-dressed Coulomb potential at the peak of the electric field. The red dashed line is $V=ER/2-I_\mathrm{p}$, while the blue dash–dotted line is $V=-ER/2-I_\mathrm{p}$. The internuclear distance is $R=12$ a.u.

The electron energy is still lower than the laser-modified barrier, which assures that tunneling dominates the ionization process. In our simulations, the internuclear distance is fixed at $R=12$ a.u. We chose this value because of the two following reasons. Firstly, H_2^+ at the equilibrium internuclear distance presents characters quite similar to atomic cases. Secondly, at $R=12$ a.u., the charge resonance enhanced ionization (CREI) takes place,[18,19] which is a typical scenario of molecular processes in strong laser fields. The initial state is obtained by imaginary time propagation.[20] The wave function is propagated with the Crank–Nicholson algorithm.[21] The space steps are $\Delta x=\Delta y=0.1$ a.u., and the time step is $\Delta t=0.025$ a.u. The simulation box has the size of 500 a.u. × 500 a.u. in the x–y coordinate space, which is big enough that no wave packet reaches the boundaries of the simulation box.

2.2. Backward propagation

To visualize the tunneling process, we propagated the photoelectron wave packet backward. To do that, after the TDSE simulation, we extracted the wave packet entering the area outside the red dashed curve shown in Fig. 2, which is regarded as the ionization part Ψ_Io. After that, we replaced the final ionized electron distribution by a classical ensemble, which was backward propagated for obtaining the tunneling exits. Numerically, we converted the ionized final state $\Psi_\mathrm{Io}(x_\mathrm{f},y_\mathrm{f})=A(x_\mathrm{f},y_\mathrm{f})\exp[\mathrm{i}S(x_\mathrm{f},y_\mathrm{f})]$ into a classical ensemble by calculating its local momentum $\boldsymbol{p}(x_\mathrm{f},y_\mathrm{f})=\nabla S(x_\mathrm{f},y_\mathrm{f})$, where $A(x_\mathrm{f},y_\mathrm{f})$ and $S(x_\mathrm{f},y_\mathrm{f})$ are the amplitude and phase, respectively. The classical trajectories in phase space $(\boldsymbol{r}(t),\boldsymbol{p}(t))$ were calculated by solving Newton equation with the initial condition $\boldsymbol{p}(x_\mathrm{f},y_\mathrm{f})$.

The fidelity of replacing a quantum wave packet distribution by its classical ensemble is calculated via:

$$f(\rho_1,\rho_2)=\frac{\int \mathrm{d}^2\boldsymbol{\xi}\sqrt{\rho_1(\boldsymbol{\xi})\rho_2(\boldsymbol{\xi})}}{\int \mathrm{d}^2\boldsymbol{\xi}\rho_1(\boldsymbol{\xi})}, \quad (4)$$

where ρ_1 and ρ_2 are the classical and quantum probability distribution with respect to momentum respectively. As already known, classical backward propagation does not produce accurate results when being used to handle the case in which severe interference occurs. In our simulation, efforts were taken to avoid such inaccuracy by neglecting the part $p_x<0$ and $A<2\times10^{-5}$.

Numerically, the tunneling is judged by the criterion that $\boldsymbol{p}$ is equal to zero along the direction of the instantaneous laser electric field, i.e.,

$$\Pi(\boldsymbol{p},\tau)=\delta(\hat{\boldsymbol{r}}\cdot\hat{\boldsymbol{p}})\delta(\tau-t), \quad (5)$$

where $\hat{\boldsymbol{r}}$ and $\hat{\boldsymbol{p}}$ are unit vectors alongside the direction of $\boldsymbol{r}$ and $\boldsymbol{p}$ respectively. The definition of tunneling exit time distribution is

$$\frac{\mathrm{d}P}{\mathrm{d}\tau}=\int \mathrm{d}^2\boldsymbol{r}_\mathrm{f}\Pi(\boldsymbol{p},\tau)A^2(\boldsymbol{r}_\mathrm{f}). \quad (6)$$

Technically, there are sometimes more than one point satisfying criterion (5). We are only interested in those x satisfying $-R/2 < x < R/2$. In our simulation, if a trajectory $(\boldsymbol{r}(t), \boldsymbol{p}(t))$ had some points between the two nuclei satisfying the criterion at some time t_1, then any point on that trajectory at $t < t_1$ would be aborted to avoid non-physical results and over-barrier ionization.

3. Results

Figure 2 shows the electron wave packet distribution after the interaction. The two nuclei locate at $(x, y) = (-6, 0)$ and $(6, 0)$. The red dashed curve marks the boundary of the bound states and free states. We propagated the wave function after the laser field vanishes until almost all ionized electron wave packets passed the dashed boundary.

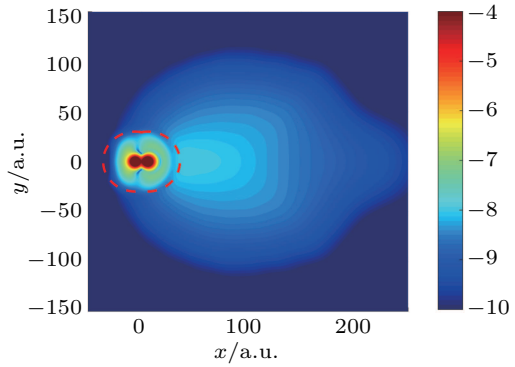


Fig. 2. (color online) Electron wave packet distribution in the logarithmic scale after the interaction. The dashed border line is formed by two circles, and each circle is centered at one of the nuclei and has a radius of 35 a.u. The wave function inside the border line is regarded as the non-ionized part, while the part outside the border line is supposed to be the ionized part. The total ionization rate calculated through this partition is 9.38×10^{-5}.

At the end of the propagation, we picked out the ionized electron wave packet, and did the fast Fourier transformation (FFT) to get the momentum distribution for the photoelectron, as shown in Fig. 3(b). Meanwhile, we show the photoelectron momentum distribution via the local momentum method in Fig. 3(a). The calculated fidelity between Fig. 3(a) and Fig. 3(b) is about 0.95, which means the classical ensemble can successfully replace the quantum results. However, a closer look of Figs. 3(a) and 3(b) shows the faint interference structures in the quantum results disappear in a classical distribution. This is the drawback of this backward propagation. Nevertheless, the momentum distribution given by the local momentum method can give the main features provided by the quantum calculations.

After having the space and momentum distribution of the photoelectron, we propagated this classical ensemble backward. When the instantaneous momentum meets the criterion of the tunneling, we recorded its position. Figure 4 shows the tunneling exits, where the two nuclear positions are represented by the two stars. As expected, the tunneling exits concentrate near the molecular bond. The tunneling exits distribute symmetrically with respect to the molecular axis, which is also within expectation. Surprisingly, the tunneling exits do not seem like a Gaussian distribution along the y axis. After looking at the laser-dressed Coulomb potential, one may find that the tunneling exit distribution shares the shape of the saddle-point distribution of the laser-dressed Coulomb potential. For other internuclear distances, for example, $R = 11$ or $R = 13$, the tunneling exit distribution does not change substantially since the ionization mechanism is still the same. One may understand the tunneling ionization more deeply after having the tunneling exits.

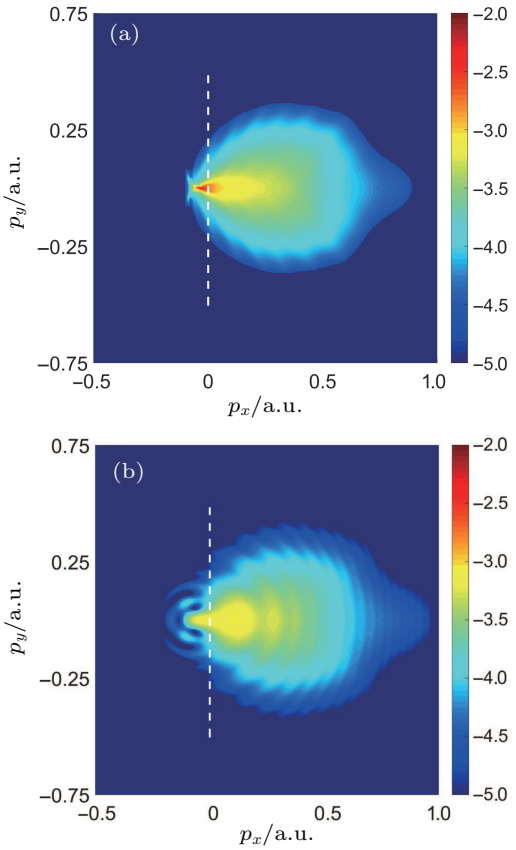


Fig. 3. (color online) Momentum distribution in the logarithmic scale obtained from (a) local momentum and (b) fast Fourier transformation (FFT). The white dashed line ($p_x = 0$) is a watershed of fidelity: on the right side of this line, interference is small enough so that local momentum roughly agrees with FFT. On the left side, they show less similarity due to the strong interference.

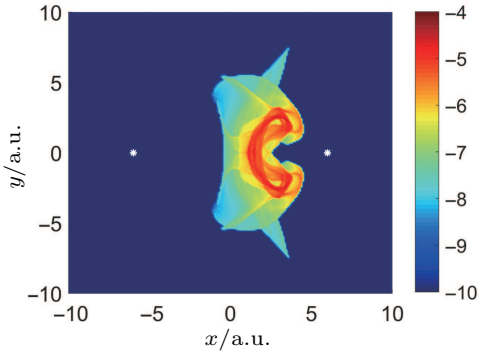


Fig. 4. (color online) The tunneling exit distribution in the logarithmic scale. The two stars in the figure represent the positions of the two nuclei. Over-barrier part and downstream ionization part occupy only 0.02% of the ionized final state, which are not shown on these two figures.

For different tunneling exits, the electron may have different angular momenta with respect to the right nucleus, as shown in Fig. 5, where ρ is the probability density as a function of L_z. For the tunneling exits in the upper and lower half spaces, the electron has opposite angular momenta, which means that the electron passes the different sides of the right nucleus.

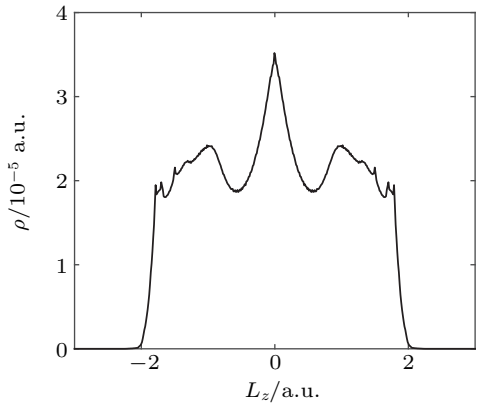


Fig. 5. Angular momentum probability distribution with respect to the downstream nucleus.

4. Conclusion

The tunneling exits of H_2^+ in strong laser fields have been studied by the TDSE simulation plus the classical backward propagation. The main tunneling exits form a moon shape, which recognizes the saddle shape of the laser-dressed Coulomb potential. Electrons tunneling out from different exits have distinct trajectories. The visualization of the tunneling exits of molecules helps understand the ultrafast dynamics of molecules in strong laser fields.

Acknowledgment

Simulations were performed on the Π supercomputer at Shanghai Jiao Tong University.

References

[1] Krausz F and Ivanov M 2009 *Rev. Mod. Phys.* **81** 163
[2] Tong Y, Jiang W C, Wu P and Peng L Y 2016 *Chin. Phys. B* **25** 073202
[3] Corkum P B 1993 *Phys. Rev. Lett.* **71** 1994
[4] Corkum P B and Krausz F 2007 *Nat. Phys.* **3** 381
[5] Keldysh L V 1965 *Sov. Phys. JETP* **20** 1307
[6] Ammosov M V, Delone N B and Krainov V P 1986 *Sov. Phys. JETP* **64** 1191
[7] Delone N B and Krainov V P 1991 *J. Opt. Soc. Am. B* **8** 1207
[8] Perelomov A M and Popov V S 1967 *Sov. Phys. JETP* **25** 336
[9] Tong X M, Zhao Z X and Lin C D 2002 *Phys. Rev. A* **66** 033402
[10] Geng J W, Xiong W H, Xiao X R, Peng L Y and Gong Q H 2015 *Phys. Rev. Lett.* **115** 193001
[11] Li M, Geng J W, Liu H, Deng Y K, Wu C Y, Peng L Y, Gong Q H and Liu Y Q 2014 *Phys. Rev. Lett.* **112** 113002
[12] Ni H C, Saalmann Ulf and Rost J M 2016 *Phys. Rev. Lett.* **117** 023002
[13] Ni H C, Saalmann Ulf and Rost J M 2018 *Phys. Rev. A* **97** 013426
[14] Wang J P and He F 2017 *Phys. Rev. A* **95** 043420
[15] He P L, Takemoto N and He F 2015 *Phys. Rev. A* **91** 063413
[16] Lao D, He P L and He F 2016 *Phys. Rev. A* **93** 063403
[17] Uiberacker M, Uphues Th, Schultze M, *et al.* 2007 *Nature* **466** 627
[18] Zuo T and Bandrauk A D 1995 *Phys. Rev. A* **52** R2511
[19] Yu Z Q, Yang W J and He F 2016 *Acta Phys. Sin.* **65** 204202 (in Chinese)
[20] Kosloff R and Kosloff D 1986 *J. Comput. Phys.* **63** 363
[21] Press W H, Teukolsky S A, Vetterling W T and Flannery B P 1992 *Numerical Recipes* (Cambridge: Cambridge University Press)